ISSN: 2476-6909; Modares. Mech. Eng. *2025;25(11):735-745.*

Modares Mechanical Engineering

DOI: 10.48311/mme.2025.116435.0
journal homepage: mme.modares.ac.ir

Cyclic Energy Absorption and Shape Recovery of Fiber-Reinforced Re-Entrant Lattice Structures: Experimental and Numerical Investigation

Shahram Hosseini, Amin Farrokhabadi*

Mechanical Engineering Department, Tarbiat Modares University, Tehran, Iran

ARTICLE INFO

Article Type
Original Research

Article History
Received: September 11, 2025
Revised: October 16, 2025
Accepted: November 01, 2025
ePublished: November 26, 2025

ABSTRACT

The development of lightweight architected lattices with superior energy absorption and recoverability is of great interest for protective systems and reusable structural components. This study investigates the mechanical performance of re-entrant auxetic lattices fabricated from pure PLA (PP) and glass-fiber-reinforced PLA composites (RP) produced via fused deposition modeling. Quasi-static compression tests were conducted to evaluate stiffness, specific energy absorption (SEA), mean crushing force, and crush force efficiency (CFE), while cyclic compression–recovery experiments assessed shape memory effects and reusability. The experimental findings were complemented by finite element simulations in ABAQUS/Explicit. Results indicate that RP structures exhibit higher stiffness, enhanced SEA, and superior CFE compared with PP counterparts, owing to improved load transfer and suppression of local buckling by reinforcing fibers. Although fiber–matrix debonding led to a temporary reduction in mean crushing force during the second cycle, RP specimens regained performance in subsequent cycles, highlighting their cyclic durability. Shape recovery tests further confirmed that RP lattices maintained higher efficiency and stability across multiple deformation–heating cycles compared with PP. The combined experimental and numerical analysis demonstrates that fiber reinforcement significantly enhances the energy absorption capability and reusability of auxetic SMP-based lattices, positioning them as promising candidates for next-generation crashworthy and impact-mitigation applications.

Keywords: Auxetic Lattices, Energy Absorption, Shape Memory Polymers, Fiber Reinforcement, Reusability

How to cite this article
Hosseini Sh, Farrokhabadi A, Cyclic Energy Absorption and Shape Recovery of Fiber-Reinforced Re-Entrant Lattice Structures: Experimental and Numerical Investigation, Modares Mechanical Engineering; *2025;25(11):735-745.*

**Corresponding author's email: amin-farrokh@modares.ac.ir*
**Corresponding ORCID ID: 0000-0002-0229-4802*

1- Introduction

The development of lightweight lattice metamaterials with enhanced energy absorption capacity has gained considerable attention in recent years, primarily due to their potential applications in impact mitigation, crashworthiness, aerospace structures, and protective devices. These structures are designed to dissipate large amounts of energy while maintaining low weight, a feature that is particularly critical in applications where both safety and structural efficiency are required. Among them, auxetic metamaterials, which are distinguished by their negative Poisson's ratio, have emerged as a promising class of structures. Unlike conventional honeycomb lattices, auxetic structures contract laterally when compressed. This behavior produces unique deformation mechanisms that improve stiffness, crushing stability, and energy absorption efficiency. Numerous studies have demonstrated the superior mechanical performance of auxetic lattices under compressive loading. Zhang and Sun [1] reported that both planar honeycombs and three-dimensional auxetic lattices exhibit higher specific energy absorption due to their stable compression process and elevated plateau stress. Their findings highlighted the potential of auxetic lattices to serve as effective buffer devices for protecting sensitive equipment and human occupants during impact events. Similarly, Bastola et al. [2] employed strut reinforcement techniques to strengthen traditional re-entrant, hexagonal, and hybrid lattice structures fabricated by additive manufacturing. Their results showed significant increases in stiffness and volumetric energy absorption, with improvements of more than 160% in some reinforced designs, confirming the effectiveness of geometric tailoring in enhancing structural performance. The applications of auxetic structures extend beyond conventional engineering components to protective equipment. Das and Kumar [3] illustrated the use of auxetic honeycomb geometries in helmet liners, where the introduction of auxetic pores substantially improved energy dissipation and reduced force transmission to the head compared with traditional helmet designs. This work demonstrated the practical relevance of auxetic lattices in safety-critical products. Along similar lines, Etemadi et al. [4] introduced re-entrant circular auxetic structures and novel variants, such as S-shaped, star, and flower configurations, fabricated via fused deposition modeling. Both experimental testing and finite element simulations confirmed that these designs outperform conventional re-entrant auxetics, particularly in terms of specific energy absorption and stress distribution, thereby widening the design possibilities for next-generation energy absorbers. Other studies have focused on introducing innovative unit-cell architectures to overcome the limitations of conventional re-entrant geometries. Esmaeili et al. [5] developed star triangular auxetic and STA-double arrow metastructures, which demonstrated distinct trade-offs between energy absorption capacity and stiffness. While the STA structure achieved nearly 20% higher energy absorption due to progressive deformation and auxeticity, the STA-DA structure provided a much higher stiffness and load-bearing capacity, emphasizing the importance of balancing different mechanical responses for targeted applications. Beyond such engineered designs, bio-inspired approaches have also proven highly promising. Ma et al. [6] proposed a lattice structure inspired by deep-sea sponge skeletons, which combined auxetic effects with superior stiffness and energy absorption compared to classical re-entrant honeycombs. Their work not only highlighted the mechanical benefits of bio-inspiration but also showed how geometrical parameters such as strut thickness and spacing critically influence auxetic response. Another recent advancement involves the development of dual-material and assemblable plate-lattice systems with auxetic behavior. Wang et al. [7] presented novel plate-lattice designs that combined hyperelastic and plastic materials in a glue-free assembly, achieving disassembly, recyclability, and enhanced mechanical properties. Their results indicated the presence of a dual-plateau stress–strain response, with the second plateau exhibiting nearly three times the stress level of the first, thereby substantially increasing the energy absorption capability of the structure. Such studies illustrate how material choice and manufacturing strategies can further complement geometric design to achieve multifunctional performance in auxetic metamaterials.

Shape memory polymers (SMPs) have recently emerged as a new class of smart materials for architected metamaterials, owing to their capability of fixing a temporary shape and subsequently recovering their permanent configuration upon exposure to external stimuli such as heat, light, magnetic field, or moisture. This phenomenon, known as the shape memory effect (SME), enables not only significant energy dissipation during deformation but also recoverability and reusability, properties that conventional polymer lattices cannot offer. The combination of SMPs with advanced manufacturing methods, particularly 3D and 4D printing, has opened new possibilities for the development of intelligent energy absorbers with programmable and reversible mechanical responses.

Recent research has demonstrated a variety of approaches for exploiting SMPs in lattice and cellular structures. Liu et al. [8] integrated magneto-responsive SMP composites into 4D-printed honeycomb and flower-like architectures, achieving rapid magnetic actuation, high shape recovery (>91%), and robust mechanical properties. Similarly, Yang et al. [9] proposed reconfigurable metamaterials fabricated from polymeric materials with mismatched moduli, enabling programmable multistability and large thermal deformations without the need for conventional thermomechanical programming. Sang et al. [10] further highlighted the reusability of SMP-based heterogeneous TPMS lattices, showing nearly complete shape recovery under thermal stimulation and stable repeated energy absorption over multiple loading cycles.

Other works have focused on improving structural robustness and multifunctionality. Li et al. [11] developed a high-performance thermoset SMP that combined excellent strength, recovery stress, recyclability, and 3D printability, enabling microlattices with mechanical properties comparable to metallic lattices but with added shape memory and self-healing functionality. Wu et al. [12] fabricated modular chiral metamaterials with SMPs that allowed programmable morphing, tunable Poisson's ratio, and active deployability in soft robotics. Likewise, Yu et al. [13] investigated multi-shape memory effects in SMPs, demonstrating that staged recovery can provide controlled energy release during deformation cycles, expanding their potential in energy management applications.

Further developments underline the versatility of SMP-based lattices for reversible energy absorption. Wang et al. [14] designed thin-walled SMP circular structures capable of progressive collapse and complete recovery after heating, enabling multiple loading–unloading cycles with consistent energy absorption capacity. Keshavarzan et al. [15] studied rhombic and BCC SMP lattices fabricated via digital light processing, showing that both could achieve high strain recovery and stable energy absorption under different programming temperatures. Hosseini et al. [16] investigated sinusoidal SMP unit cells under repeated quasi-static loading, reporting that while absorbed energy decreased slightly with each cycle, the structures retained their shape recovery capability and remained effective energy absorbers across multiple deformation–heating cycles.

Beyond these studies, several other works have further enriched the understanding and applications of SMP-based metamaterials. Pokras et al. [17] demonstrated the feasibility of fabricating multi-material lattice structures using commercially available thermoplastic polyurethane (TPU) SMPs via fused deposition modeling, highlighting their potential for 4D printing and broader accessibility. Pirhaji et al. [18] investigated the thermomechanical response of octet-truss SMP lattices with ultra-low densities, showing that relative density and pre-strain are key parameters governing stress recoverability and energy absorption behavior. Yan and Li [19]

developed a constitutive modeling framework to predict the thermomechanical behavior of SMP lattices across multiple length scales, confirming that structural hierarchy can significantly enhance load-bearing and energy absorption capabilities. Roudbarian et al. [20] explored triply periodic minimal surface (TPMS) lattices made from SMPs, revealing how micro-architecture and volume fraction influence shape fixity, recovery, and elastic modulus, thereby suggesting biomedical applications such as patient-specific implants. Other innovative approaches have focused on coupling SMPs with additional functionalities. Yu et al. [21] presented transformable SMP-based lattices capable of fracture healing and reversible configuration changes, enabling structures with tunable stiffness, vibration, and acoustic properties. Wang et al. [22] proposed SMP-based thin-walled structures with cyclic reversible energy absorption under varying thermal conditions. Additionally, they reviewed electrospun SMP fibers (SMPFs), pointing to their multifunctionality in biomedical scaffolds, sensors, smart textiles, and energy harvesting. Collectively, these studies broaden the design space for SMP-based architectures, ranging from energy absorbers to healable, reconfigurable, and multifunctional devices.

The pursuit of lightweight architected materials that offer exceptional energy dissipation and functional durability has become a central theme in advanced composites and additive manufacturing research. These materials, particularly lattice structures, are pivotal for applications ranging from personal protection to aerospace components. This review synthesizes recent advancements in the design, analysis, and performance of cellular structures, with a focus on their energy absorption characteristics and the transformative role of fiber reinforcement and multi-material design. A significant body of work has been dedicated to exploring the mechanical and energy-absorbing properties of various lattice topologies. Gharehbaghi et al. [23] experimentally and numerically investigated the energy absorption in honeycomb structures based on lozenge grid unit cells, finding that the loading angle significantly influences performance, with the highest capacity at 0° or 90°. Similarly, Hosseinpour et al. [24] studied the energy absorption of thin-walled auxetic cylindrical tubes, demonstrating the profound effect of porosity variation on their crushing behavior. Extending this to a novel design, Zhu et al. [25] proposed a 3D-printed cutting-type energy-absorbing structure from short carbon fiber-reinforced polyamide, achieving remarkable specific energy absorption through a combination of extrusion and shearing mechanisms, highlighting a different route to crashworthiness.

The investigation of auxetic structures, known for their negative Poisson's ratio and potential for superior conformity, has been another key area. Mohammadi Ghalehney et al. [26] focused on 2D re-entrant gradient structures produced by additive manufacturing, demonstrating their potential to reduce stress shielding in bone implants by creating a modulus gradient. This work was expanded upon by Mohammadi Ghalehney et al. [27], who integrated a genetic algorithm to optimize an auxetic gradient structure for a hip joint implant, showcasing a sophisticated approach to tailoring mechanical properties for specific biomedical applications.

The integration of fiber reinforcement into these architected materials has been widely recognized as a critical method for enhancing their mechanical properties. Ghorbani et al. [28] developed an analytical model using the energy method to evaluate the equivalent properties of bone-inspired cellular structures, confirming that continuous fiber reinforcement yields significantly higher stiffness and strength. Complementing this, Farrokhabadi et al. [29] utilized Classical Laminate Theory (CLT) to predict the mechanical properties of 3D-printed honeycombs, also noting the superior energy absorption of foam-filled variants and the benefit of commingled yarns. For dynamic scenarios, Avarzamani et al. [30] evaluated functionally graded sinusoidal cellular structures under compression, revealing that the energy absorption superiority of a specific geometry is dependent on the loading direction, a crucial consideration for anisotropic designs. Beyond static and quasi-static properties, the long-term and cyclic performance of these composite lattices is essential for reusable applications. Gharehbaghi et al. [31] provided critical insights into the fatigue behavior of continuous glass fiber-reinforced PLA honeycombs, developing S-N curves and analyzing the degradation of residual stiffness and strength, which directly informs predictions of service life under cyclic loads. From a structural mechanics perspective, Gharehbaghi et al. [32] employed Hyperbolic Shear Deformable Beam Theory (HSDBT) to enhance the analytical accuracy in evaluating the mechanical properties of a new hexagonal pyramid unit cell, accounting for shear effects that are often significant in lattice structures.

Collectively, previous studies have demonstrated that SMP-based metamaterials can overcome the permanent deformation limitations of conventional polymer lattices and introduce functionalities such as reusability, self-healing, and programmable shape recovery. Their integration with re-entrant and other architected geometries has made them promising candidates for adaptive and energy-absorbing systems. However, despite these advancements, the combined effect of fiber reinforcement and cyclic shape recovery in auxetic SMP lattices has not been systematically investigated. Previous works have typically focused either on improving the mechanical strength of polymer lattices through fiber addition or on exploring the shape recovery characteristics of pure SMP structures. The interaction between these two mechanisms—load transfer by reinforcing fibers and recoverability driven by the shape memory effect—remains largely unexplored, particularly under repeated deformation and recovery cycles.

The novelty of the present work lies in integrating fiber reinforcement with shape memory behavior within re-entrant auxetic lattices to achieve enhanced stiffness, energy absorption capacity, and cyclic recoverability. The study experimentally and numerically investigates the mechanical response and recovery performance of fiber-reinforced re-entrant lattices fabricated via fused deposition modeling (FDM). The findings provide new insights into designing lightweight, reusable, and durable energy-absorbing structures for crashworthiness and impact-mitigation applications.

2- Problem statement

In this study, a re-entrant unit cell was selected as the fundamental building block for designing energy absorbers. The geometry of the unit cell is illustrated in Fig. 1. Despite extensive research on auxetic and shape memory polymer (SMP)-based lattice structures, most existing studies have focused on either geometric optimization or thermal recovery behavior in isolation. The combined influence of fiber reinforcement on the cyclic energy absorption and shape recovery of re-entrant lattices has not been systematically investigated. In particular, there is a lack of studies integrating experimental testing with finite element simulations to assess how reinforcement affects stiffness, plateau stability, and recoverability over multiple compression–heating cycles. Therefore, the present study aims to fill this gap by developing and analyzing fiber-reinforced re-entrant auxetic lattices fabricated via fused deposition modeling, and by examining their mechanical response, energy absorption capability, and cyclic durability both experimentally and numerically.

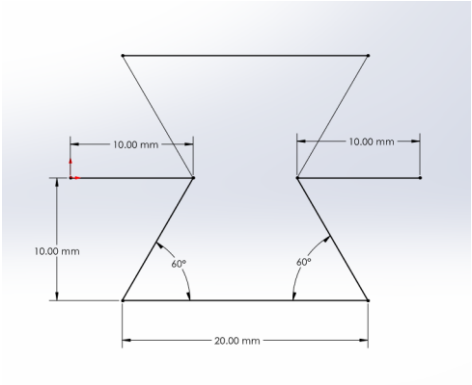

Fig. 1 Geometry of the re-entrant unit cell used in this study

To generate an auxetic lattice structure, the re-entrant unit cell was periodically expanded along both the horizontal and vertical directions. The resulting 2D auxetic lattice configuration, derived from the unit cell, is shown in Fig. 2.

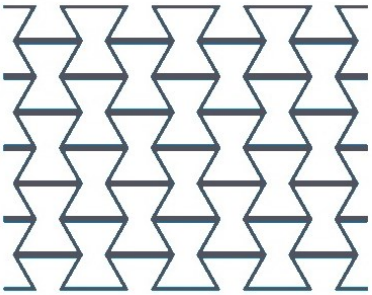

Fig. 2 Periodically expanded re-entrant auxetic lattice structure based on the unit cell

3- Experimental Analysis

3-1- 3D printing

In this study, the experimental specimens were fabricated using a Fused Deposition Modeling (FDM) 3D printer. This additive manufacturing method was chosen due to its capability to produce complex geometries with high precision and cost-effectiveness. Moreover, FDM provides the possibility of fabricating fiber-reinforced composites, enabling the integration of reinforcement during the printing process.

The printing parameters employed in this study are summarized in Table 1. These parameters were optimized to ensure dimensional accuracy, proper interlayer adhesion, and consistent mechanical performance of the fabricated structures.

Table 1 Printing parameters used for fabricating the experimental specimens

parameter	Value
Nozzle Diameter	**1 mm**
Filament Diameter	**1.75 mm**
Nozzle Temperature	**200ºC**
Bed Temperature	**50 ºC**
Print speed	**3mm/s**
Height of layer	**0.32 mm**

The printing parameters listed in Table 1 were selected based on a series of preliminary tests and prior studies on FDM-printed PLA composites to ensure optimal print quality and mechanical consistency. The nozzle and bed temperatures (200 °C and 50 °C, respectively) were chosen to promote proper filament flow and interlayer adhesion while preventing thermal degradation or warping. A layer height of 0.32 mm and print speed of 3 mm/s provided a balance between dimensional accuracy and fabrication time, minimizing void formation and ensuring uniform fiber impregnation in composite samples. These conditions yielded stable extrusion and reproducible specimen geometry for subsequent mechanical testing.

3-1-1- Tensile test sample

To determine the baseline mechanical properties of the raw material, tensile test specimens were fabricated in accordance with the ASTM D638 Type IV standard. The geometry of the specimen is illustrated in Fig. 3. These standardized samples were printed using the same process parameters described in Table 1 to ensure consistency between the tensile tests and the structural samples.

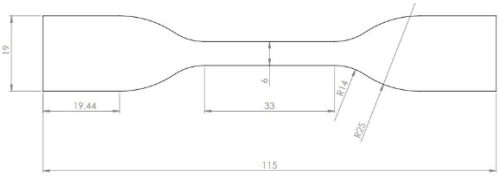

Fig. 3 Geometry of the ASTM D638 Type IV tensile test specimen.

3-1-2- Pure PLA re-entrant sample

The pure PLA re-entrant structures were fabricated to serve as the reference configuration. The geometry of the re-entrant unit cell and its periodic arrangement were first designed in a CAD software and subsequently imported into Cura slicing software. The final models were printed using the parameters listed in Table 1. This ensured that the PLA specimens exhibited consistent surface quality, dimensional accuracy, and layer adhesion, which are critical for reliable mechanical testing.

3-1-3- Composite re-entrant sample

To enhance the mechanical performance of the lattice structures, fiber-reinforced re-entrant samples were fabricated using an in-situ impregnation method. In this process, the thermoplastic filament was impregnated with reinforcing fibers prior to extrusion, allowing the formation of composite filaments during printing. This technique improves stiffness, strength, and energy absorption capacity by ensuring uniform fiber distribution and effective bonding with the polymer matrix.

This approach provides several advantages:

1. Preservation of fiber integrity and length, which results in superior stiffness and strength compared to short-fiber composites.

2. Unprecedented flexibility in controlling key parameters such as Fiber Volume Ratio and fiber pathing, which can be dynamically adjusted during the printing process.

3. Possibility of topology optimization, enabling the fabrication of high-performance components with material distributed only in regions where it is structurally required.

For the fabrication of the composite samples, the re-entrant geometry was first designed in a CAD software. The corresponding G-code was then generated in Cura slicing software, and the final printing was performed using the parameters listed in Table 1. The fabricated composite re-entrant lattice structure is shown in Fig. 5.

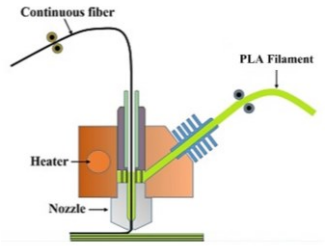

Fig. 5 Fiber-reinforced re-entrant composite lattice fabricated using the in-situ impregnation method.

3-2- Extracting Mechanical properties

To obtain the mechanical properties of PLA, tensile tests were conducted on 3D-printed specimens in accordance with the ASTM D638 standard. The specimens were fabricated using the same FDM parameters listed in Table 1 to ensure consistency between the test samples and the structural specimens. During testing, the samples were subjected to uniaxial tensile loading at a crosshead speed of 5 mm/min, as prescribed by the ASTM standard. The measured stress–strain data were then used to extract the fundamental mechanical parameters, including Young's modulus, yield strength, and ultimate tensile strength. These properties served as input values for both the finite element simulations and the experimental analysis of the re-entrant lattices.

Fig. 6 uniaxial tensile test for extracting mechanical properties

The experimentally obtained mechanical properties of the 3D-printed PLA material are summarized in Table 2. These values were used as input parameters for the finite element simulations described in Section 4. The results indicate that the fabricated PLA specimens exhibit mechanical properties consistent with those reported in the literature for FDM-printed thermoplastic polymers, confirming the reliability of the printing and testing procedure.

Table 2 Mechanical properties of 3D-printed PLA obtained from ASTM D638 tensile tests.

Property	Symbol	Average value	Unit
Young's modulus	E	2.35	**GPa**
Yield stress	σ_y	52.4	**MPa**
Ultimate tensile stress	σ_u	61.8	**MPa**
Elongation at break	ε_u	5.7	**%**

3-3- Quasi-static analysis

To evaluate the energy absorption behavior of the fabricated structures, quasi-static compression tests were performed on both pure PLA samples and fiber-reinforced composite samples. The specimens were subjected to uniaxial compressive loading at a constant displacement rate of 5 mm/min, following standard practices for energy absorber characterization.

The applied load and corresponding displacement were continuously recorded, allowing the generation of force–displacement curves for each specimen. From these curves, key energy absorption parameters, such as stiffness, specific energy absorption (SEA), mean crushing force, and crush force efficiency (CFE), were calculated. These parameters provide a quantitative basis for comparing the performance of different lattice configurations and material compositions.

3-4- Shape Recovery Analysis

One of the most attractive features of shape memory polymers is their ability to recover their original configuration after undergoing large plastic deformations when exposed to appropriate thermal stimuli. This property not only enhances the reusability of the material but also contributes to its long-term energy absorption capability, making SMP-based lattices promising candidates for reversible protective structures.

In this study, the shape recovery behavior of the re-entrant lattice structures was investigated through cyclic loading–unloading tests. Initially, each specimen was subjected to quasi-static compression up to about 30% strain, corresponding to the onset of densification and representing significant plastic deformation. After unloading, the deformed specimen was placed under a controlled thermal condition to trigger the shape recovery process.

The recovered sample was then subjected to repeated compression tests, and its energy absorption performance was re-evaluated after each cycle. This procedure was repeated three times to assess the repeatability of recovery, the extent of dimensional restoration, and the influence of glass fiber reinforcement on both recovery efficiency and energy absorption behavior.

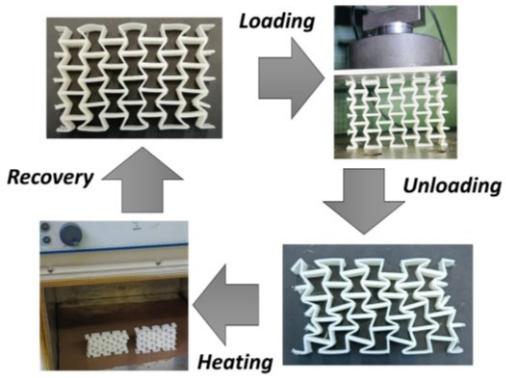

Fig. 6 Shape-recovery testing sequence for the re-entrant lattice

4- FEM Analysis

To validate the experimental findings, numerical simulations were carried out using the finite element software ABAQUS/Explicit. The Dynamic Explicit solver was selected due to its robustness in handling large deformations and nonlinear contact interactions during compression of lattice structures.

For the pure PLA samples, the mechanical properties obtained from the ASTM D638 tensile tests (Section 3.2) were directly assigned to the material model. For the glass-fiber-reinforced composite samples, the properties of glass fibers were adapted from [33]. The composite models were developed by representing the polymer matrix and reinforcing fibers separately, with their respective mechanical properties assigned individually. The interaction between the matrix and fibers was modeled using an ideal tie constraint, ensuring perfect bonding between the two phases. This assumption allows for a simplified representation of load transfer and is commonly adopted in FEA of short-fiber and continuous-fiber composites. The developed FE models provide a reliable framework for comparing load–

displacement responses, deformation modes, and energy absorption performance with the experimental results.

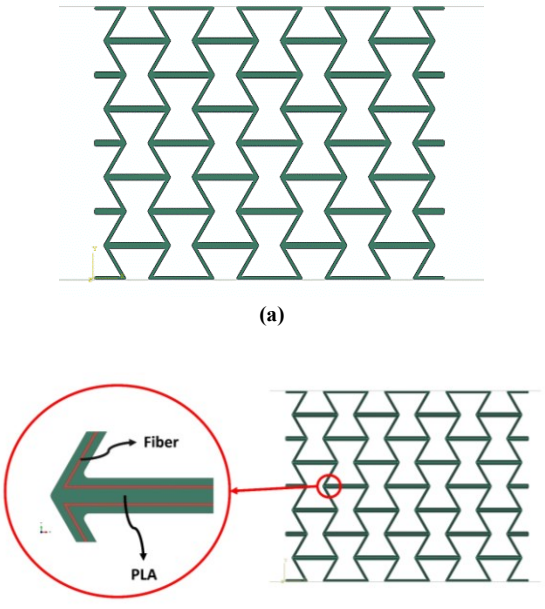

Fig. 7 Finite element model of the re-entrant lattice: (a) pure PLA sample, (b) glass-fiber-reinforced composite with separate matrix and fiber phases

It should be noted that the assumption of perfect bonding between the fibers and the polymer matrix, implemented through a tie constraint, represents a simplification of the actual interfacial behavior. In practice, local debonding or interfacial slip may occur under cyclic loading, which can influence the stress transfer and energy absorption response of the composite lattice. Nevertheless, this assumption was adopted to ensure numerical stability and computational efficiency, and because interfacial parameters for the printed composite were not experimentally determined in the present study. Future work will consider more advanced interfacial models, such as cohesive zone elements or debonding criteria, to capture the fiber–matrix interaction more accurately.

5- Energy absorption parameters

To evaluate the performance of the energy absorbers, compare their behavior, and identify the most effective configuration, several parameters can be examined. These are discussed in the following sections.

The first parameter investigated in this study is stiffness, defined as the structure's resistance to deformation under applied loading. It plays a critical role in the energy absorption performance and is also referred to as the equivalent elastic modulus. This parameter directly influences the mechanical behavior of the absorber, stress distribution, and the amount of energy absorbed. It is calculated using the following relation:

$$E_{eq} = \frac{\Delta F_{linear}}{\Delta x_{linear}} \quad (1)$$

where ΔF_{linear} denotes the change in force within the linear region of the force–displacement curve, and Δx_{linear} is the corresponding displacement.

The next parameter is Specific Energy Absorption (SEA). SEA is a critical parameter in materials and structural engineering, representing the efficiency of energy absorption per unit mass of a structure or material. It is especially important in the design of systems where high energy absorption must be achieved with minimal weight, such as in automotive, aerospace, or protective equipment applications. SEA is calculated using the following relation:

$$SEA = \frac{\int F dx}{m} \quad (2)$$

where m represents the mass of the structure.

Another important parameter in evaluating energy absorbers is the mean force, which represents the average force exerted on the structure throughout the deformation process. This parameter indicates the average amount of force required for the structure to absorb energy during deformation and is calculated using the following relation:

$$P_{mean} = \frac{\int F dx}{x_{end}} \quad (3)$$

where x_{end} denotes the onset of the densification phase.

A further critical parameter in energy absorber analysis is the Crush Force Efficiency (*CFE*), which reflects the uniformity of the structure's compression under loading. *CFE* is used to assess how effectively a structure can absorb energy without generating dangerous stress peaks, and is calculated as:

$$CFE = \frac{P_{mean}}{P_{peak}} \times 100 \quad (4)$$

where P_{peak} represents the initial peak force in the force–displacement curve. A *CFE* value closer to 100% indicates a more stable deformation process with no sudden structural failures.

Energy Absorption Efficiency refers to the efficiency with which energy is absorbed throughout the deformation process. This metric illustrates how effectively a structure or material can convert the input energy into deformation or other mechanical responses without experiencing rapid or severe failure. The Energy Absorption Efficiency at point a is computed using the following expression:

$$\eta(x_a) = \frac{\int_0^{x_a} F(x) dx}{F(x_a)} \quad (5)$$

6- Results and Discussion

In this section, the experimental and numerical results obtained from the quasi-static compression tests and finite element simulations are presented and discussed in detail. The primary objective of this analysis is to evaluate the mechanical response, energy absorption performance, and shape recovery capability of the re-entrant lattice structures fabricated from pure PLA (PP) and glass-fiber-reinforced PLA composites (RP).

Fig. 8 presents the load–displacement response of the two types of lattices, namely PP and RP, under quasi-static compression loading. This figure allows us to compare the initial stiffness, peak load, and energy absorption capacity between the two configurations.

For the PP, the response shows a relatively lower initial slope and a smaller peak load, followed by a plateau region with noticeable fluctuations. These oscillations are associated with local buckling and progressive collapse of the struts, leading to less stable energy absorption. In contrast, the RP exhibits a steeper initial slope, a higher peak force, and a more stable plateau region, which indicates improved load transfer and delayed onset of densification due to the presence of reinforcing fibers. From an energy absorption perspective, the composite structure not only dissipates more energy within the same displacement range but also reduces sudden force drops, thereby improving crush force efficiency.

Fig. 9 illustrates representative deformation stages of the re-entrant lattices under quasi-static compression for the PP and the RP. As compression progresses, PP displays pronounced local buckling and progressive collapse of individual struts, which leads to irregular folding patterns and localized material fragmentation; these local

failures produce the force oscillations observed in the force–displacement response. By contrast, RP deforms in a more coordinated manner: the reinforcing fibers bridge cracked regions and increase the flexural stiffness of struts, which delays the onset of catastrophic local buckling and promotes the formation of more regular folding bands across the lattice. Consequently, RP preserves load-bearing paths longer, shows fewer abrupt drops in load during compression, and achieves a more gradual transition to the densification stage. These distinct damage modes explain the superior mean crushing force and improved plateau stability of the composite configuration, while also suggesting different post-failure energy dissipation mechanisms.

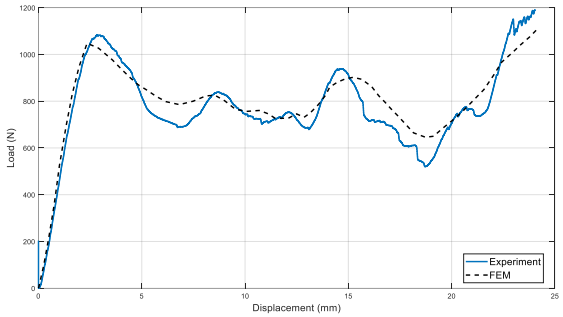

(a)

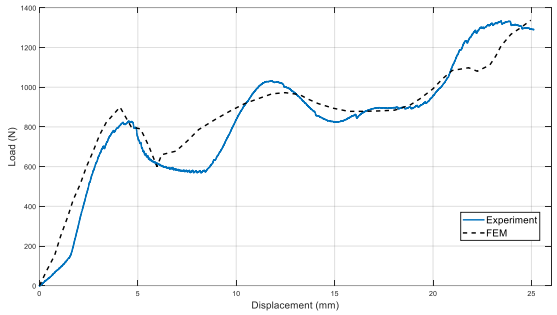

(b)

Fig. 8 Load–displacement curves of re-entrant lattice structures under quasi-static compression using FEM and Experimental analysis for (a) pure PLA, and (b) glass-fiber-reinforced composite

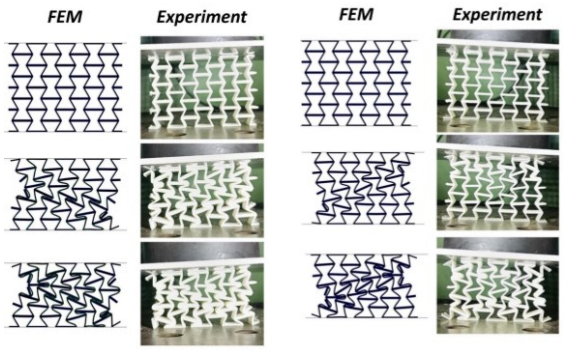

(a) (b)

Fig. 9 Sequential deformation snapshots of re-entrant lattices under quasi-static compression: (a) pure PLA, and (b) glass-fiber-reinforced composite

Fig. 10 compares the cyclic compression–recovery behavior of the PP and RP lattices. In the first loading cycle, both structures exhibit their characteristic load–displacement responses, but the differences between the two become more pronounced in subsequent cycles after thermal recovery. The PP shows a reduction in peak force and plateau stability with each cycle, indicating partial damage accumulation and limited recovery of the original geometry. This degradation reflects the intrinsic limitations of neat PLA, which lacks sufficient structural reinforcement to fully restore load-bearing capability after repeated deformation. In contrast, the RP demonstrates much better retention of stiffness and plateau force across cycles. The reinforcing fibers provide structural bridging and constrain localized plastic deformation, thereby enabling the lattice to recover a larger portion of its initial mechanical performance after each recovery step. As a result, RP has more stable plateau regions even after multiple cycles. These results emphasize that while both materials benefit from the shape recovery process, the composite configuration achieves superior cyclic durability, making it more suitable for reusable energy absorption applications.

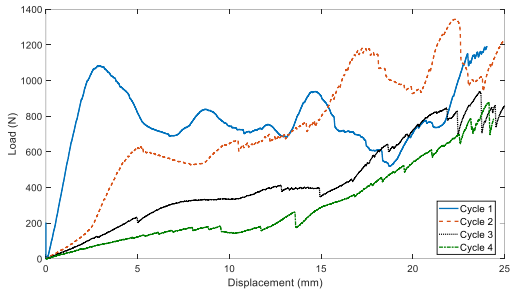

(a)

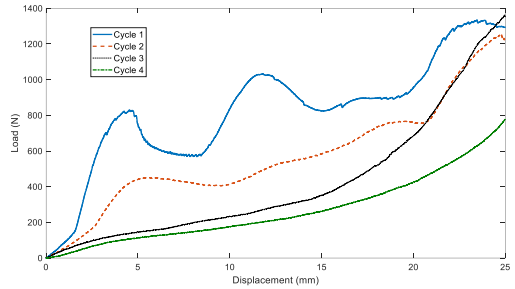

(b)

Fig. 10 Cyclic compression–recovery responses of re-entrant lattices: comparison between M1 (pure PLA) and M2 (glass-fiber-reinforced composite) over repeated loading cycles.

Fig. 11 illustrates the Energy Absorption Efficiency of the re-entrant lattices for both the PP and the RP under quasi-static compression. For PP, the efficiency curve rises during the early stages of deformation but shows clear fluctuations in the plateau region. These oscillations correspond to localized strut buckling and unstable collapse mechanisms, which reduce the overall efficiency of energy absorption. In contrast, the RP exhibits a smoother and more stable Efficiency profile, with consistently higher values across most of the deformation process. The improved efficiency of RP is a direct consequence of fiber reinforcement, which stabilizes the deformation mode, delays localized failures, and distributes stresses more uniformly throughout the lattice. This behavior highlights the superior capacity of the composite structure to absorb and manage energy in a controlled manner, making it a more reliable option for applications where stable energy dissipation is critical.

Fig. 12 shows the equivalent elastic modulus (E_{eq}) measured for PP and RP across four compression–recovery cycles. Although the RP exhibits a lower E_{eq} than the PP in the first cycle, the subsequent cycles reveal a markedly different trend: the E_{eq} of the PP decreases more rapidly with cycling, while the composite's modulus is much more stable and the difference between the two materials narrows by cycle four. This behavior indicates that the RP undergoes less structural degradation during compression and thermal recovery, likely because

the reinforcing fibers preserve load paths, limit localized plasticity and crack growth, and therefore reduce the relative loss of stiffness over repeated use. The result highlights the superior cyclic durability of the composite configuration for reusable energy-absorbing applications.

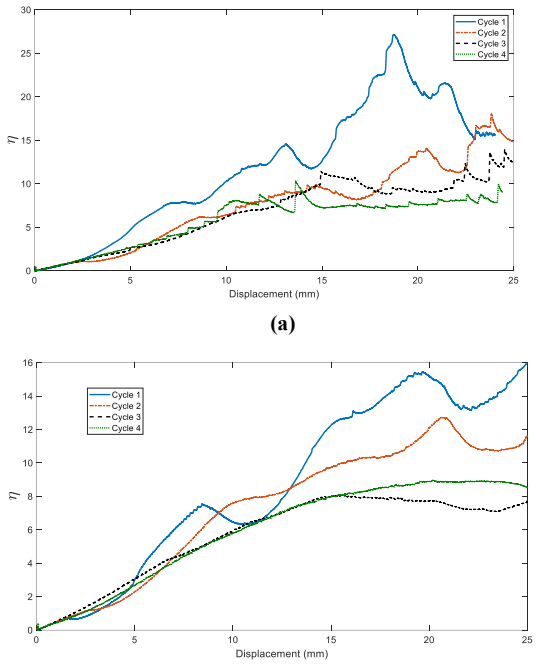

Fig. 11 Comparison of energy absorption efficiency between (a) pure PLA, and (b) glass-fiber-reinforced composite lattices under quasi-static compression.

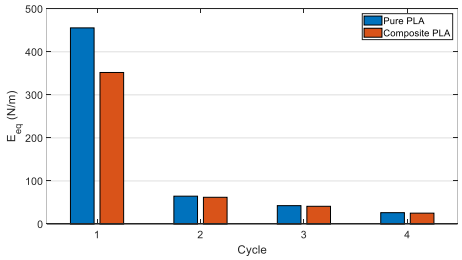

Fig. 12 Equivalent elastic modulus for pure PLA and composite PLA over four compression–recovery cycles (Cycle 1–Cycle 4).

Fig. 13 presents the variation of Specific Energy Absorption for PP and RP over four consecutive compression–recovery cycles. As can be seen, the specific energy absorption of RP is higher than that of PP, and despite the higher mass of RP compared to PP (m_{pp} = 44 gr, m_{rp} = 45.2 gr), its specific energy absorption is greater, indicating the positive effect of using reinforcing fibers in this structure. It is also observed that even under the second to fourth loading cycles, the energy absorption of the RP structure remains higher.

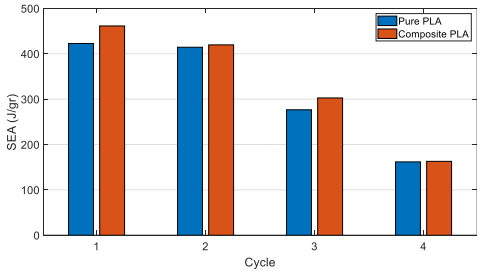

Fig. 13 Specific Energy Absorption for pure PLA and composite PLA over four compression–recovery cycles (Cycle 1–Cycle 4).

To provide a clearer quantitative comparison between the two material configurations, the specific energy absorption (SEA) values obtained from the experiments are summarized in Table 3. As seen, the SEA of the fiber-reinforced composite (RP) is consistently higher than that of pure PLA (PP) across all four compression–recovery cycles, confirming the beneficial effect of fiber reinforcement on the energy absorption capability and cyclic durability of the lattice structure.

Table 3 Specific Energy Absorption (SEA) values of pure PLA (PP) and fiber-reinforced PLA (RP) re-entrant lattices across four consecutive compression–recovery cycles.

Cycle	SEA (PP) [J/gr]	SEA (RP) [J/gr]
1	422.65	461.33
2	414.41	419.6
3	276.51	302.64
4	161.65	162.87

Fig. 14 presents the mean load values of the PP and RP specimens under different loading cycles. As can be seen, the P_{mean} values of the RP structure are higher than those of PP in the first cycle, indicating the superior performance of RP. In the second cycle, this value experiences a more pronounced reduction for RP, which reflects the lower load required to initiate the energy absorption process. This significant decrease can be attributed to the occurrence of fiber–matrix debonding at certain regions, which reduces the required load for subsequent energy absorption. However, during the third and fourth cycles, a recovery in the mean load of RP specimens is observed, demonstrating the improved performance of this structure. Therefore, in the first cycle, the presence of reinforcing fibers plays a positive role; in the second cycle, due to fiber–matrix debonding, the performance decreases; and in the third and fourth cycles, the performance improves again.

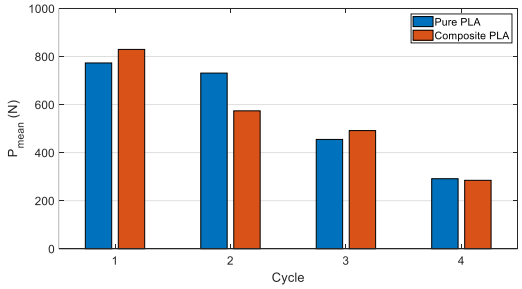

Fig. 14 Mean force for pure PLA and composite PLA over four compression–recovery cycles (Cycle 1–Cycle 4).

Fig. 15 illustrates the Crush Force Efficiency of RP and PP specimens across different loading cycles. As observed, this parameter exhibits a considerably higher value for RP compared to PP during the first loading cycle, indicating a more uniform energy absorption behavior of the RP specimen. Moreover, in the second to fourth cycles, this superiority of RP over PP remains evident.

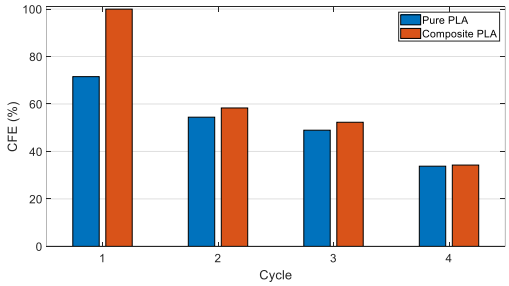

Fig. 15 Crush Force Efficiency for pure PLA and composite PLA over four compression–recovery cycles (Cycle 1–Cycle 4).

7- Conclusion

This study presented a comprehensive experimental and numerical analysis of re-entrant auxetic lattice structures fabricated from pure PLA and fiber-reinforced PLA composites. The results demonstrated that fiber reinforcement not only increases stiffness and specific energy absorption but also stabilizes the crushing response by delaying local buckling and reducing force oscillations. Among the evaluated parameters, SEA and CFE of RP specimens consistently outperformed those of PP, even under repeated compression–recovery cycles. Although fiber–matrix debonding caused a reduction in mean crushing force during the second cycle, subsequent cycles revealed recovery of structural performance, underscoring the durability of the composite configuration. Furthermore, shape memory effects enabled RP lattices to retain superior energy absorption efficiency and modulus stability over multiple cycles, confirming their potential for reusable protective systems. Overall, the integration of reinforcing fibers into auxetic SMP-based lattices offers a viable pathway for developing lightweight, efficient, and reusable energy absorbers for crashworthiness, aerospace, and impact-mitigation applications. Although the present study provides a comprehensive evaluation under quasi-static loading, it does not include high strain-rate or impact tests, which are essential for assessing real-world crashworthiness. Moreover, the thermal recovery behavior was examined under controlled laboratory conditions, and environmental effects such as humidity and long-term cyclic fatigue were not considered. Future research will address these aspects by investigating dynamic and impact responses, temperature-dependent viscoelastic effects, and optimization of fiber orientation and content to enhance energy absorption and recovery efficiency.

Beyond the fundamental findings, the results of this study have direct implications for practical engineering applications. The demonstrated combination of high energy absorption, stiffness stability, and recoverability makes the proposed fiber-reinforced SMP lattices promising candidates for lightweight crashworthy components, impact energy absorbers in vehicles, reusable protective gear, and vibration-damping elements in aerospace structures. Moreover, the ability to recover shape and mechanical performance after multiple deformation–heating cycles suggests potential for recyclable and sustainable designs in future engineering products. These attributes collectively position the proposed concept as a viable solution for next-generation adaptive and reusable protective systems.

Ethics Approval:

The scientific content of this article is the result of the authors' research and has not been published in any Iranian or international journal.

Conflict of Interest:

There is no conflict of interest to declare.

Funding:

This work is based upon research funded by Iran National Science Foundation (INSF) under project No.403224

References

[1] Q. Zhang and Y. Sun, "Energy absorption characteristic of auxetic metamaterials honeycombs and lattices with negative thermal expansion," *Thin-Walled Struct.*, vol. 208, no. September 2024, p. 112824, 2025, DOI: 10.1016/j.tws.2024.112824.

[2] N. Bastola, J. Ma, and M. P. Jahan, "Enhancing mechanical and energy absorption properties of additively manufactured polyamide lattice structures through hybrid-structuring and strut reinforcement: a numerical and experimental study," *Int. J. Adv. Manuf. Technol.*, vol. 136, no. 5, pp. 2397–2426, 2025, DOI: 10.1007/s00170-024-14907-8.

[3] R. Das and G. S. Kumar, "Auxetic Honeycomb Lattice Structure in Thin Solids for Enhanced Energy Absorption: Innovative Two-Wheeler Helmet Design and Analysis," *Comput. Aided. Des. Appl.*, vol. 21, no. 6, pp. 1136–1148, 2024, DOI: 10.14733/cadaps.2024.1136-1148.

[4] E. Etemadi, M. Hosseinabadi, M. Taghizadeh, F. Scarpa, and H. Hu, "Enhancing the energy absorption capability of auxetic metamaterials through auxetic cells within re-entrant circular units," *Eng. Struct.*, vol. 315, no. June, p. 118379, 2024, DOI: 10.1016/j.engstruct.2024.118379.

[5] A. Esmaeili, M. Karimi, M. Heidari-Rarani, and M. Shojaie, "A new design of star auxetic metastructure with enhanced energy-absorption under various loading rates: Experimental and numerical study," *Structures*, vol. 63, no. April, pp. 2023–2024, 2024, DOI: 10.1016/j.istruc.2024.106457.

[6] J. Ma, H. Zhang, T. U. Lee, H. Lu, Y. M. Xie, and N. S. Ha, "Auxetic behavior and energy absorption characteristics of a lattice structure inspired by deep-sea sponge," *Compos. Struct.*, vol. 354, no. September 2024, p. 118835, 2025, DOI: 10.1016/j.compstruct.2024.118835.

[7] W. J. Wang, W. M. Zhang, M. F. Guo, H. Yang, and L. Ma, "Impact resistance of assembled plate-lattice auxetic structures," *Compos. Struct.*, vol. 338, no. December 2023, 2024, DOI: 10.1016/j.compstruct.2024.118132.

[8] H. Liu, F. Wang, W. Wu, X. Dong, and L. Sang, "4D printing of mechanically robust PLA/TPU/Fe3O4 magneto-responsive shape memory polymers for smart structures," *Compos. Part B Eng.*, vol. 248, no. August 2022, p. 110382, 2023, DOI: 10.1016/j.compositesb.2022.110382.

[9] H. Yang, N. D'Ambrosio, P. Liu, D. Pasini, and L. Ma, "Shape memory mechanical metamaterials," *Mater. Today*, vol. 66, no. June, pp. 36–49, 2023, DOI: 10.1016/j.mattod.2023.04.003.

[10] L. Sang *et al.*, "Reusability and energy absorption behavior of 4D-printed heterogeneous lattice structures based on biomass shape memory polyester," *J. Mater. Res. Technol.*, vol. 27, pp. 1563–1578, 2023, DOI: 10.1016/j.jmrt.2023.09.323.

[11] A. Li, A. Challapalli, and G. Li, "4D Printing of Recyclable Lightweight Architectures Using High Recovery Stress Shape Memory Polymer," *Scientific Reports*, vol. 9, no. 1. 2019. DOI: 10.1038/s41598-019-44110-9.

[12] Y. Wu, Y. Han, Z. Wei, Y. Xie, J. Yin, and J. Qian, "4D Printing of Chiral Mechanical Metamaterials with Modular Programmability using Shape Memory Polymer," *Adv. Funct. Mater.*, vol. 33, no. 52, pp. 1–2, 2023, DOI: 10.1002/adfm.202306442.

[13] K. Yu, T. Xie, J. Leng, Y. Ding, and H. J. Qi, "Mechanisms of multi-shape memory effects and associated energy release in shape memory

polymers," *Soft Matter*, vol. 8, no. 20, pp. 5687–5695, 2012, DOI: 10.1039/c2sm25292a.

[14] K. Wang, G. Sun, J. Wang, S. Yao, M. Baghani, and Y. Peng, "Reversible energy absorbing behaviors of shape-memory thin-walled structures," *Eng. Struct.*, vol. 279, no. January, p. 115626, 2023, DOI: 10.1016/j.engstruct.2023.115626.

[15] M. Keshavarzan, M. Kadkhodaei, and F. Forooghi, "An investigation into compressive responses of shape memory polymeric cellular lattice structures fabricated by vat polymerization additive manufacturing," *Polym. Test.*, vol. 91, no. August, p. 106832, 2020, DOI: 10.1016/j.polymertesting.2020.106832.

[16] S. Hosseini, A. Farrokhabadi, and D. Chronopoulos, "Experimental and numerical analysis of shape memory sinusoidal lattice structure: Optimization through fusing an artificial neural network to a genetic algorithm," *Compos. Struct.*, vol. 323, no. August, p. 117454, 2023, DOI: 10.1016/j.compstruct.2023.117454.

[17] D. Pokras, Y. Schneider, S. Zaidi, and V. K. Viswanathan, "Shape Memory Polymers in 4D Printing: Investigating Multi-Material Lattice Structures," *Journal of Manufacturing and Materials Processing*, vol. 8, no. 4. 2024. DOI: 10.3390/jmmp8040154.

[18] A. Pirhaji, E. Jebellat, N. Roudbarian, K. Mohammadi, M. R. Movahhedy, and M. Asle Zaeem, "Large deformation of shape-memory polymer-based lattice metamaterials," *Int. J. Mech. Sci.*, vol. 232, p. 107593, Oct. 2022, DOI: 10.1016/J.IJMECSCI.2022.107593.

[19] C. Yan and G. Li, *Design oriented constitutive modeling of amorphous shape memory polymers and Its application to multiple length scale lattice structures*, vol. 28, no. 9. 2019. DOI: 10.1088/1361-665X/ab230c.

[20] N. Roudbarian, E. Jebellat, S. Famouri, M. Baniasadi, R. Hedayati, and M. Baghani, "Shape-memory polymer metamaterials based on triply periodic minimal surfaces," *Eur. J. Mech. A/Solids*, vol. 96, no. May, p. 104676, 2022, DOI: 10.1016/j.euromechsol.2022.104676.

[21] K. Yu *et al.*, "Healable, memorizable, and transformable lattice structures made of stiff polymers," *NPG Asia Mater.*, vol. 12, no. 1, 2020, DOI: 10.1038/s41427-020-0208-9.

[22] L. Wang, F. Zhang, Y. Liu, and J. Leng, "Shape Memory Polymer Fibers: Materials, Structures, and Applications," *Adv. Fiber Mater.*, vol. 4, no. 1, pp. 5–23, 2022, DOI: 10.1007/s42765-021-00073-z.

[23] H. Gharehbaghi, M. Jamshidi, and A. Almomani, "Experimental and numerical investigation of energy absorption in honeycomb structures based on lozenge grid unit cells under various loading angles," *Compos. Part C Open Access*, vol. 15, no. November, p. 100546, 2024, DOI: 10.1016/j.jcomc.2024.100546.

[24] E. Hosseinpour, A. Moazemi, and F. Morshedsolouk, "Numerical and experimental study on the energy absorption characteristics of thin-walled auxetic cylindrical tubes with varying porosity," *J. Mater. Res. Technol.*, vol. 39, no. September, pp. 400–417, 2025, DOI: 10.1016/j.jmrt.2025.09.135.

[25] W. Zhu *et al.*, "Design and crashworthiness behaviors of novel 3D printed cutting-type energy-absorbing composite structures," *Mech. Adv. Mater. Struct.*, vol. 6494, 2025, DOI: 10.1080/15376494.2025.2476207.

[26] S. Mohammadi Ghalehney, M. H. Sadeghi, and H. Gharehbaghi, "Mechanical Properties of 2D Re-Entrant Gradient Structures Produced by Additive Manufacturing," *Iran. J. Sci. Technol. - Trans. Mech. Eng.*, vol. 48, no. 3, pp. 1395–1404, 2024, DOI: 10.1007/s40997-023-00724-z.

[27] S. Mohammadi Ghalehney, M. H. Sadeghi, H. Barati, and H. Gharehbaghi, "Enhancing auxetic gradient structures for hip joint implants to optimize stress shielding reduction," *Phys. Scr.*, vol. 99, no. 11, 2024, DOI: 10.1088/1402-4896/ad818e.

[28] F. Ghorbani, H. Gharehbaghi, A. Farrokhabadi, and A. Bolouri, "Investigation of the equivalent mechanical properties of the bone-inspired composite cellular structure: Analytical, numerical and experimental approaches," *Compos. Struct.*, vol. 309, no. September 2024, pp. 2024–2025, 2023, DOI: 10.1016/j.compstruct.2023.116720.

[29] A. Farrokhabadi, H. Gharehbaghi, H. Malekinejad, M. Sebghatollahi, Z. Noroozi, and H. Veisi, "Study of Equivalent Mechanical Properties and Energy Absorption of Composite Honeycomb Structures," *Int. J. Appl. Mech.*, vol. 15, no. 6, pp. 1–2, 2023, DOI: 10.1142/S1758825123500382.

[30] M. Avarzamani, H. Gharehbaghi, M. Bahrami, A. Farrokhabadi, A. H. Behravesh, and S. K. Hedayati, "Energy absorption response of functionally graded 3D printed continuous fiber reinforced composite cellular structures: Experimental and numerical approaches," *Mech. Adv. Mater. Struct.*, vol. 32, no. 4, pp. 538–554, 2025, DOI: 10.1080/15376494.2024.2352036.

[31] H. Gharehbaghi, A. M. Shojaei, M. Sadeghzadeh, and A. Farrokhabadi, "Residual stiffness and strength analysis of fatigue behavior in a 3D-printed honeycomb structure of continuous glass fiber-reinforced polylactic acid (PLA) composite," *Compos. Part C Open Access*, vol. 16, no. December 2024, p. 100552, 2025, DOI: 10.1016/j.jcomc.2024.100552.

[32] H. Gharehbaghi and A. Farrokhabadi, "Analytical, experimental, and numerical evaluation of mechanical properties of a new unit cell with hyperbolic shear deformable beam theory," *Mech. Adv. Mater. Struct.*, vol. 31, no. 25, pp. 6419–6433, 2024, DOI: 10.1080/15376494.2023.2231441.

[33] Y. Jeong, H. Kim, J. Kim, J. Kim, S. Kim, and J. Lee, "Results in Engineering Evaluation of mechanical properties of glass fiber-reinforced composites depending on length and structural anisotropy," *Results Eng.*, vol. 17, no. February,

p. 101000, 2023, DOI: 10.1016/j.rineng.2023.101000.